Infinite Class of $\mathcal{PT}$-Symmetric Theories from One Timelike Liouville Lagrangian

Carl M. Bender,[1,2,3,*] Daniel W. Hook,[1,4,†] Nick E. Mavromatos,[2,5,‡] and Sarben Sarkar[2,§]
[1]Department of Physics, Washington University, St. Louis, Missouri 63130, USA
[2]Department of Physics, King's College London, London WC2R 2LS, United Kingdom
[3]Department of Mathematical Science, City University London, Northampton Square, London EC1V 0HB, United Kingdom
[4]Department of Physics, Imperial College London, London SW7 2AZ, United Kingdom
[5]Theory Division, CERN, CH-1211 Geneva 23, Switzerland
(Received 14 August 2014; published 3 December 2014)

Logarithmic timelike Liouville quantum field theory has a generalized $\mathcal{PT}$ invariance, where $\mathcal{T}$ is the time-reversal operator and $\mathcal{P}$ stands for an S-duality reflection of the Liouville field ϕ. In Euclidean space, the Lagrangian of such a theory $L = \frac{1}{2}(\nabla\phi)^2 - ig\phi\exp(ia\phi)$ is analyzed using the techniques of $\mathcal{PT}$-symmetric quantum theory. It is shown that L defines an infinite number of unitarily inequivalent sectors of the theory labeled by the integer n. In one-dimensional space (quantum mechanics), the energy spectrum is calculated in the semiclassical limit and the mth energy level in the nth sector is given by $E_{m,n} \sim (m+1/2)^2 a^2/(16n^2)$.

DOI: 10.1103/PhysRevLett.113.231605 PACS numbers: 03.70.+k, 03.65.-w, 11.30.Er

Two-dimensional conformal field theories have attracted enormous attention in the physics community, in part because of their role as the underlying world-sheet theory of (first quantized) strings and in part because they describe one-space-dimensional systems, such as spin chains, which are of great interest in condensed matter physics. At the boundary between two-dimensional conformal field theories and general (renormalizable) two-dimensional field theories lie the so-called Liouville field models, which also describe the gravitational sector of strings away from their conformal points in theory space [1–6]. Upon analytic continuation in the Liouville mode, the so-called timelike Liouville theories are obtained. Such models may be used either as regulators [7] that aid in understanding the nonperturbative structure of correlation functions of Liouville models [8] or as toy models for quantum gravity effects in inflation [9] and in the dark energy and acceleration of the Universe. Quantum-mechanical models based on timelike Liouville field theories [7,10] have been studied in the semiclassical limit, where the central charge (counting degrees of freedom) tends to infinity. Such works shed light on the structure of correlation functions of the full field theories.

Motivated by studies of timelike logarithmic Liouville quantum field theory, we examine here the interaction $-ig\phi\exp(ia\phi)$ in field theory and its quantum-mechanical analog $-igx\exp(iax)$. This remarkable interaction gives rise to a countably infinite number of inequivalent quantum theories.

The interaction $-ig\phi\exp(ia\phi)$ has its origin in conformal field theory (CFT) of the Liouville type, whose interaction has the form $e^{\alpha\phi}$ [1–6]. This exponential arises in string theory and in two-dimensional gravity, which are defined on two-dimensional manifolds. Using general coordinate invariance, one can show that the metric tensor $g_{\mu\nu}$ for these theories can be reduced locally to $g_{\mu\nu} = \eta_{\mu\nu}e^{\alpha\phi}$, where $\eta_{\mu\nu}$ is the Minkowski metric. String theory and two-dimensional gravity are conformally invariant at the classical level, but quantum effects can produce an anomaly that destroys conformal invariance. Conformal symmetry is restored if the field ϕ is governed by the Liouville action

$$S = \int_{-\infty}^{\infty} d\tau \int_0^{2\pi} d\sigma \left[\frac{1}{2}(\partial_\tau\phi)^2 - \frac{1}{2}(\partial_\sigma\phi)^2 - ge^{\alpha\phi}\right].$$

Recoil effects for zero-dimensional D-branes scattering off closed strings are described by the interaction $\phi e^{\alpha\phi}$ in addition to the usual Liouville interaction $e^{\alpha\phi}$ [11]. Such pairs of operators define a logarithmic CFT [12]. Logarithmic CFTs also arise in descriptions of quenched disordered condensed matter systems [13,14]. Supercritical strings [15] and the condensation of tachyons [7,16] are studied in the context of timelike Liouville theories, whose interaction term has α replaced by ia. Thus, combining the ideas of Liouville and logarithmic CFT, we are led to consider the d-dimensional Euclidean Lagrangian

$$L = \frac{1}{2}(\nabla\phi)^2 - ig\phi e^{ia\phi} - he^{ia\phi}, \tag{1}$$

where ϕ is a scalar field and a, g, and h are treated as positive-real parameters.

The Lagrangian (1) is not Hermitian, and one cannot make such a theory Hermitian by adding its Hermitian conjugate because this would destroy the conformality property of the theory. Nevertheless, the techniques of $\mathcal{PT}$ quantum theory [17] can be used to study this field theory. The Lagrangian is not obviously $\mathcal{PT}$ invariant because in Liouville theory the field ϕ is assumed to transform as a scalar, so it does not change sign under space reflection. [If ϕ were a pseudoscalar field, the Lagrangian would be $\mathcal{PT}$ invariant because under parity reflection $\mathcal{P}$, ϕ would

 © 2014 American Physical Society

change sign $\mathcal{P}\phi(x,t)\mathcal{P} = -\phi(-x,t)$, and under time reversal $\mathcal{T}$, i changes sign $\mathcal{T}i\mathcal{T} = -i$.] However, we let $\mathcal{P}$ represent an S-duality reflection [18]

$$\mathcal{P}\phi(x,t)\mathcal{P} = -\phi(x,t), \tag{2}$$

and with this definition of $\mathcal{P}$, L is manifestly $\mathcal{PT}$ symmetric. A non-Hermitian $\mathcal{PT}$-invariant theory can have a positive-real spectrum and unitary time evolution [17].

The interaction terms of Eq. (1) have a periodic component, and thus L bears a resemblance to some previously studied $\mathcal{PT}$-symmetric theories, including the complex Toda lattice [19], complex diffraction gratings [20], and complex crystal lattices [21]. Complex $\mathcal{PT}$-symmetric periodic potentials exhibit a real-energy band structure. There have also been studies of the complex sine-Gordon equation [22], complex dynamical systems [23], and $\mathcal{PT}$-symmetric exponential potentials [24]. However, the factor of ϕ multiplying g in Eq. (1), which is characteristic of logarithmic CFT, leads to surprising new effects. Specifically, the partition function as a path integral over L

$$Z_n = \int \mathcal{D}\phi \exp\left(\int d^d x\, L\right) \tag{3}$$

has *infinitely* many distinct functional integration paths labeled by $n = 1, 2, 3\ldots$, each defining a valid but unitarily *inequivalent* quantum theory. This multiplicity of theories is not due to monodromy (there is no winding number because the integrand is entire) nor is it a topological effect (like θ vacua). The quantum-mechanical version of this timelike logarithmic CFT has discrete energy levels rather than energy bands. The mth energy level in the nth theory grows like m^2 as $m \to \infty$, but for fixed m the energies decay like n^{-2} as $n \to \infty$.

To find the integration paths on which the integral (3) converges, we must locate in field space the pairs of Stokes wedges inside which the integrand vanishes exponentially. To begin, we simplify this integral by shifting ϕ by a constant to eliminate the parameter h in L. Next, we neglect the effect of the kinetic term $(\nabla\phi)^2$ because it does not affect the convergence. We also ignore the spatial integral in the exponent and study the convergence at each lattice point separately; that is, we perform an *ultralocal* analysis [25] and examine the convergence of

$$I = \int d\phi \exp(ig\phi e^{ia\phi}). \tag{4}$$

We illustrate how to locate Stokes wedges in the complex-ϕ plane by using monomial potentials ϕ^k. For such potentials the angular opening of the Stokes wedges has a simple k dependence. For $k = 4$ the integral $\int d\phi \exp(-\phi^4)$ converges in a pair of Stokes wedges of angular opening 45° centered about the positive-ϕ and negative-ϕ axes (Fig. 1, left panel). The integration contour must terminate inside these Stokes wedges. For a $\mathcal{PT}$-symmetric upside-down $-\phi^4$ potential, the associated integral $\int d\phi \exp(\phi^4)$ converges in a pair of Stokes wedges of angular opening 45° centered about $\arg\phi = -45°$ and $\arg\phi = -135°$ (Fig. 1, right panel).

The integral I in Eq. (4) is unusual because it converges in pairs of Stokes wedges of asymptotic angular opening 0°. There are infinitely many such Stokes wedges in the complex-ϕ plane, all parallel to the negative-imaginary axis. Each pair of wedges defines a distinct physical theory having its own real-energy spectrum. Guralnik and Pehlevan [26] first recognized that for functional integrals, inequivalent classes of contours with different complex boundary conditions are associated with nonunique solutions to the Dyson-Schwinger equations. They found that multiple solutions account for inequivalent θ vacua [26]. In Ref. [27] it was shown that if the pairs of Stokes wedges possess left-right symmetry ($\mathcal{PT}$ symmetry) in complex field space, the field theory is physically acceptable because the masses (poles of the Green's functions) are real and the theory is unitary. However, Ref. [27] only considered the case of a *finite* number of distinct physical theories, one theory for each pair of wedges.

Here, we consider the unusual case of an infinite number of inequivalent theories corresponding to pairs of infinitely thin Stokes wedges. To find the paths of integration on which I converges, we introduce polar coordinates $\phi = Re^{i\theta}$ and treat R as large. Then, Eq. (4) becomes

$$I = \int d\phi \exp(igRe^{-aR\sin\theta}e^{i\theta + iaR\cos\theta}). \tag{5}$$

We need to find Stokes wedges, that is, the angles at which the integrand vanishes exponentially fast as $R \to \infty$. At the center θ of a Stokes wedge, the exponent in Eq. (5) must be *real*, and thus $\theta + aR\cos\theta \sim (n + 1/2)\pi$ as $R \to \infty$ (n integer). Also, the argument of the exponential must be *negative* so that it vanishes as $R \to \infty$. Thus, $\sin(\theta + aR\cos\theta) \sim 1$ as $R \to \infty$, and we find that

$$\theta + aR\cos\theta \sim (\pm 2n + 1/2)\pi \quad (R \to \infty), \tag{6}$$

where $n > 0$. The *maximum* rate of decay occurs at the center of the wedge, so θ must be close to $-\pi/2$. Hence, we substitute $\theta = -\pi/2 + \epsilon$ into Eq. (6) and obtain $\epsilon \sim (2n+1)\pi/(aR)$ $(R \to \infty)$. We find that the centers of the Stokes wedges lie at

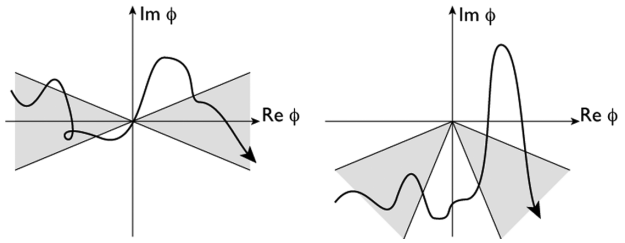


FIG. 1. Integration paths terminating in Stokes wedges (shaded regions) for Hermitian ϕ^4 (left panel) and $\mathcal{PT}$-symmetric $-\phi^4$ (right panel) interactions.

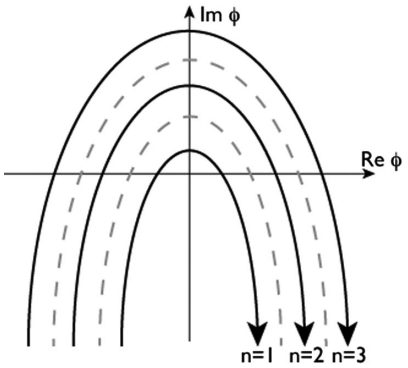


FIG. 2. Integration paths in complex-ϕ space for which the integral (4) converges. The paths terminate in infinitely thin Stokes wedges and define unitarily inequivalent theories.

$$\theta_n \sim -\frac{1}{2}\pi \pm \frac{(2n+1)\pi}{aR} \quad (R \to \infty). \tag{7}$$

To summarize for the partition function Z_n in Eq. (3), the nth path of functional integration originates in the $-n$th Stokes wedge, terminates in the nth Stokes wedge, and is asymptotically parallel to the negative-imaginary axis. The path is $\mathcal{PT}$ (left-right) symmetric (see Fig. 2).

The $\mathcal{PT}$-symmetric quantum-mechanical Hamiltonian $\mathcal{H}$ corresponding to the field-theoretic Lagrangian (1) is

$$\mathcal{H} = p^2 - igxe^{iax} + he^{iax}, \tag{8}$$

where a, g, and h are assumed to be real and positive. As we did for the the field-theoretic model, we shift x by a constant to eliminate h and obtain the Hamiltonian

$$\mathcal{H} = p^2 - igxe^{iax}. \tag{9}$$

Both quantum-mechanical Hamiltonians (8) and (9) possess a singular limit. If $a \to 0$, $\mathcal{H}$ in Eq. (9) reduces to $\mathcal{H} = p^2 - igx$. This limit is singular because, as was shown by Herbst, the spectrum of this Hamiltonian is null [28]. To explain intuitively the absence of eigenvalues, we solve Hamilton's classical equations $\dot{x} = \partial\mathcal{H}/\partial p = 2p$, $\dot{p} = -\partial\mathcal{H}/\partial x = ig$. Combining these equations gives $\ddot{x} = 2ig$, whose solutions are parabolas in the complex plane: $x(t) = igt^2 + \alpha t + \beta$. ($\alpha$ and β are constants.) Parabolas are *open* curves (see Fig. 3), so it is not possible to satisfy the Bohr-Sommerfeld (WKB) quantization condition $\oint dx\sqrt{E - V(x)} = (m + 1/2)\pi \quad (m = 0, 1, 2\ldots)$, which involves an integral over a *closed* path.

A singular limit of $\mathcal{H}$ in Eq. (8) is $g \to 0$, which gives the Hamiltonian $\mathcal{H} = p^2 + he^{iax}$ studied in Refs. [20,21]. This Hamiltonian exhibits real-energy bands but has no discrete energies. To explain intuitively the absence of discrete eigenvalues, we plot the classical paths in the complex plane (see Fig. 4). We see that these classical paths are 2π periodic and thus are open curves.

In contrast, the classical paths for $\mathcal{H}$ in Eq. (9) are closed (see Fig. 7). Thus, that Hamiltonian has discrete bound states. To prepare for calculating the eigenvalues of the bound states of $\mathcal{H}$ in Eq. (9), we must locate the classical turning points, which are the roots of $E = -igxe^{iax}$. We assume that E, g, and a are all positive and let $x = A + iB$. Thus, we must solve the transcendental equation

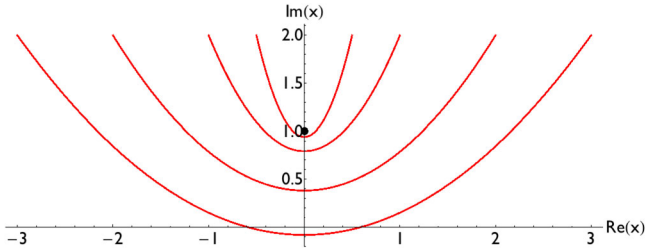


FIG. 3 (color online). Complex classical paths for the potential $V = -ix$ with $E = 1$. The paths are parabolic and thus do not close.

$$E = -ig(A + iB)e^{ia(A+iB)}. \tag{10}$$

The imaginary part of Eq. (10) gives B in terms of A, $B = A\cot(aA)$, and substituting this result into Eq. (10) gives $E\sin(aA)/(gA) = e^{-aA\cot(aA)}$. So, if we let $\nu = aE/g$ and $\alpha = aA$, we get the transcendental equation

$$\nu\alpha^{-1}\sin\alpha = e^{-\alpha\cot\alpha}. \tag{11}$$

To solve this equation graphically, we plot the left side of Eq. (11) as a solid curve and the right side as a dotted curve. (The left and right sides are even functions of x.) The intersections of these curves are solutions to Eq. (11).

Figure 5 shows that there are two sets of solutions. The first is exactly $x = n\pi$, but we reject this solution because it gives $B = \infty$. The second set has intersection points near $\alpha_n = (2n + 1/2)\pi - \delta$, where $\delta \ll 1$ as $n \to \infty$. Thus, for large n the turning points are located symmetrically about the imaginary-x axis at

$$\begin{aligned} \mathrm{Re}x &= A \sim \pm(2n + 1/2)\pi/a, \\ \mathrm{Im}x &= B \sim \frac{1}{a}\log\left[\frac{(2n + 1/2)\pi g}{aE}\right]. \end{aligned} \tag{12}$$

Table I verifies the accuracy of this asymptotic formula.

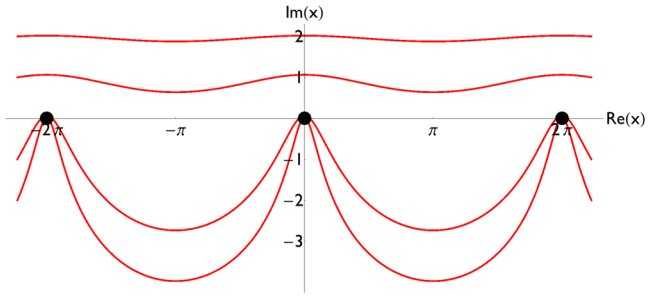


FIG. 4 (color online). Classical paths for $H = \frac{1}{2}p^2 + e^{ix}$ at $E = 1$. The classical paths are 2π periodic and open.

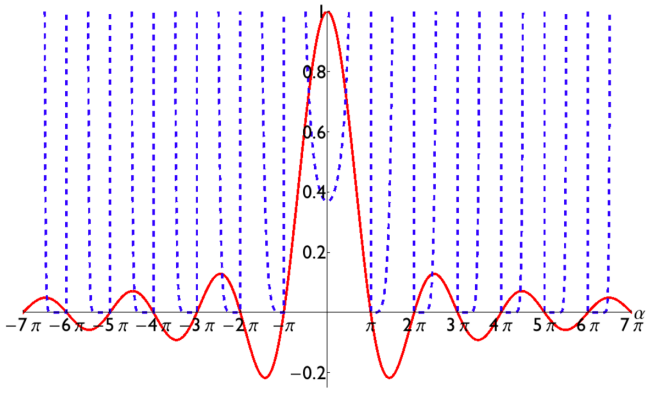


FIG. 5 (color online). Graphical solution to Eq. (11). The solid curve is the left side of Eq. (11), and the dashed curve is the right side.

Having found the turning points, we next examine the complex classical paths for $\mathcal{H}$ in Eq. (9). In general, for any given Hamiltonian, the classical energy determines a continuous family of classical paths distinguished by the initial value of x. See, for example, the classical paths for the x^2 oscillator in Fig. 6 (left panel) and for the x^6 oscillator in Fig. 6 (right panel). Note that every family of classical paths encloses one pair of turning points.

The classical paths for the Hamiltonian (9) are shown in Fig. 7. The turning points are enclosed in pairs. Also shown are the separatrix paths (see Table II) that divide the families of closed classical trajectories.

Finally, we perform a leading-order WKB calculation of eigenvalues of the Hamiltonian in Eq. (9). In general, when a theory is quantized, each pair of classical turning points (and its continuous family of closed complex classical paths) corresponds to a different and unitarily inequivalent quantum theory. For example, the central pair of turning points in Fig. 6 (right panel) corresponds to the conventional Hermitian x^6 quantum oscillator, whereas the upper and lower pairs correspond to $\mathcal{PT}$-symmetric x^6 oscillators. Thus, since there are an infinite number of pairs of classical turning points for the model in Fig. 7, we anticipate that there will be an infinite number of classes of eigenvalues for the time-independent Schrödinger equation for $\mathcal{H}$ in Eq. (9)

$$-\psi''(x) - igxe^{iax}\psi(x) = E\psi(x). \tag{13}$$

TABLE I. Good agreement between the numerically precise values of the turning points and the asymptotic approximation in Eq. (12) when $a = 1$, $g = 1$, and $E = 1$.

Turning point number	Exact	Approximate
$n = 0$	$1.3372 + 0.3181i$	$1.5708 + 0.4516i$
$n = 1$	$7.5886 + 2.0623i$	$7.8540 + 2.0610i$
$n = 2$	$13.9492 + 2.6532i$	$14.1372 + 2.6488i$
$n = 3$	$20.2725 + 3.0202i$	$20.4204 + 3.0165i$
$n = 4$	$26.5805 + 3.2878i$	$26.7035 + 3.2848i$

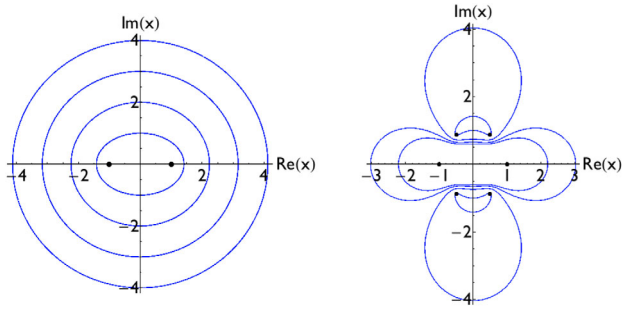


FIG. 6 (color online). Left panel: Four complex classical paths for the $p^2 + x^2$ oscillator with energy $E = 1$. The family of paths encloses the turning points (dots) at $x = \pm 1$ and fills the entire complex plane. Right panel: Two examples of each of the three families of classical paths for the $p^2 + x^6$ oscillator for $E = 1$. Each family encloses one pair of turning points, and together the three families fill the complex plane.

The complex-x WKB quantization condition is

$$\int_{x_{-n}}^{x_n} dx\sqrt{E + igxe^{iax}} = (m + 1/2)\pi, \tag{14}$$

where the turning points $x_{\pm n} = (1/a)[\pm 2n\pi + i\log(2n\pi g/aE)]$ are given in Eq. (12). For large n, Eq. (14) simplifies to

$$\frac{(m + 1/2)a}{2n\sqrt{E}} \sim \int_{-1}^{1} dw\sqrt{1 + iwe^{2in\pi w}} \sim 2(n \to \infty).$$

Thus, for large n and large m, the WKB approximation to the mth energy in the nth eigenspectrum is

$$E_{m,n} \sim (m + 1/2)^2 a^2 n^{-2}/16. \tag{15}$$

The mth eigenvalue in the nth spectrum grows like the energies in a square well [30]. However, the mth eigenvalue in the nth spectrum behaves like the energy levels in the Balmer series for the hydrogen atom and decays like n^{-2}. The parameter g does not appear in Eq. (15); it appears only in higher-order WKB. The theories corresponding to different values of n are all inequivalent—they are associated with different pairs of Stokes wedges and have different energy spectra. To conclude, $\mathcal{PT}$ analysis reveals

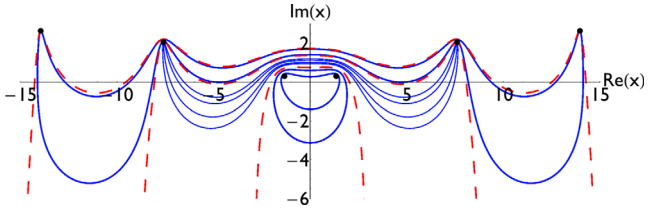


FIG. 7 (color online). Classical paths (solid curves) and separatrices (dashed curves) for $\mathcal{H}$ in Eq. (9) for $a = 1$, $g = 1$, and $E = 1$. The central paths enclose the $n = \pm 1$ pair of turning points (dots); the next family encloses the $n = \pm 2$ pair, and so on.

TABLE II. Points where the separatrix paths in Fig. 7 cross the imaginary axis [29].

Number of separatrix	Crossing point on the y axis
$n = 1$	$0.7613i$
$n = 2$	$1.3867i$
$n = 3$	$1.7485i$

the simple but astonishing structure that underlies timelike Liouville logarithmic CFT.

In future work, we will investigate (i) whether it is possible to tunnel between the inequivalent theories that we have found, which in toy cosmological applications as in Ref. [9] may correspond to an exit from the inflationary phase, and (ii) whether it is possible to examine the (nonperturbative) conformal nature of two-dimensional logarithmic CFT by studying the WKB approximation to the quantum-mechanical eigenfunctions in Eq. (13) [10].

C. M. B. was supported in part by the U.S. Department of Energy, and N. E. M. was supported in part by the London Centre for Terauniverse Studies (LCTS), using funding from the European Research Council via the Advanced Investigator Grant No. 267352 and by Science and Technology Facilities Council (STFC) (U.K.) under the Research Grant No. ST/J002798/1. C. M. B. and S. S. are grateful for a Royal Society (U.K.) International Exchange Grant.

*cmb@wustl.edu
†d.hook@imperial.ac.uk
‡nikolaos.mavromatos@kcl.ac.uk
§sarben.sarkar@kcl.ac.uk

[1] A. M. Polyakov, Phys. Lett. **103B**, 207 (1981); A. M. Polyakov, Mod. Phys. Lett. A **02**, 893 (1987).
[2] E. Braaten, T. Curtright, and C. Thorn, Ann. Phys. (N.Y.) **147**, 365 (1983).
[3] F. David, Mod. Phys. Lett. A **03**, 1651 (1988).
[4] J. Distler and H. Kawai, Nucl. Phys. **B321**, 509 (1989).
[5] N. Seiberg, Prog. Theor. Phys. Suppl. **102**, 319 (1990).
[6] Y. Nakayama, Int. J. Mod. Phys. A **19**, 2771 (2004).
[7] D. Harlow, J. Maltz, and E. Witten, J. High Energy Phys. 12 (2011) 071.
[8] M. Goulian and M. Li, Phys. Rev. Lett. **66**, 2051 (1991); H. Dorn and H. J. Otto, Nucl. Phys. **B429**, 375 (1994); A. B. Zamolodchikov, arXiv:hep-th/0505063; I. K. Kostov and V. B. Petkova, Teor. Mat. Fiz. **146**, 132 (2006) [Theor. Math. Phys. **146**, 108 (2006)]; I. K. Kostov and V. B. Petkova, Nucl. Phys. **B770**, 273 (2007); I. K. Kostov and V. B. Petkova, Nucl. Phys. **B769**, 175 (2007); G. Giribet, Phys. Rev. D **85**, 086009 (2012); A. B. Zamolodchikov and A. B. Zamolodchikov, Nucl. Phys. **B477**, 577 (1996).
[9] E. J. Martinec and W. E. Moore, J. High Energy Phys. 07 (2014) 053.
[10] W. McElgin, Phys. Rev. D **77**, 066009 (2008).
[11] N. E. Mavromatos and I. I. Kogan, Phys. Lett. B **375**, 111 (1996).
[12] V. Gurarie, Nucl. Phys. **B410**, 535 (1993).
[13] J. Cardy, J. Phys. A **46**, 494001 (2013).
[14] J.-S. Caux, I. I. Kogan, and A. M. Tsvelik, Nucl. Phys. **B466**, 444 (1996).
[15] N. E. Mavromatos, in *From Fields to Strings: Circumnavigating Theoretical Physics*, edited by M. Shifman, A. Vainshtein, and J. F. Wheater (World Scientific, Singapore, 2005), Vol. II, p. 1257.
[16] A. Strominger and T. Takayanagi, Adv. Theor. Math. Phys. **7**, 369 (2003).
[17] C. M. Bender, Rep. Prog. Phys. **70**, 947 (2007).
[18] L. O'Raifeartaigh, J. M. Pawlowski, and V. V. Sreedhar, Ann. Phys. (N.Y.) **277**, 117 (1999).
[19] T. Hollowood, Nucl. Phys. **B384**, 523 (1992).
[20] M. V. Berry and D. H. J. O'Dell, J. Phys. A **31**, 2093 (1998).
[21] A $\mathcal{PT}$-symmetric crystal is described by the non-Hermitian $\mathcal{PT}$-symmetric Hamiltonian $H = p^2 + i\sin x$, which has real-energy bands. The wave function for a particle in such a crystal is bosonic (2π periodic) at both edges of the conduction band, whereas the wave function for an ordinary Hermitian crystal is fermionic (4π periodic) at one edge and bosonic at the other edge. See C. M. Bender, G. V. Dunne, and P. N. Meisinger, Phys. Lett. A **252**, 272 (1999).
[22] C. M. Bender, H. F. Jones, and R. J. Rivers, Phys. Lett. B **625**, 333 (2005).
[23] C. M. Bender, D. D. Holm, and D. W. Hook, J. Phys. A **40**, F81 (2007); C. M. Bender, D. C. Brody, and D. W. Hook, J. Phys. A **41**, 352003 (2008); T. Arpornthip and C. M. Bender, Pramana J. Phys. **73**, 259 (2009); C. M. Bender, D. W. Hook, and K. S. Kooner, J. Phys. A **43**, 165201 (2010); A. G. Anderson, C. M. Bender, and U. I. Morone, Phys. Lett. A **375**, 3399 (2011); A. G. Anderson and C. M. Bender, J. Phys. A **45**, 455101 (2012).
[24] T. Curtright and A. Veitia, J. Math. Phys. (N.Y.) **48**, 102112 (2007).
[25] E. R. Caianiello and G. Scarpetta, Nuovo Cimento Soc. Ital. Fis. **22A**, 448 (1974).
[26] G. Guralnik and C. Pehlevan, Nucl. Phys. **B811**, 519 (2009); G. Guralnik and C. Pehlevan, Nucl. Phys. **B822**, 349 (2009); Z. Guralnik and G. S. Guralnik, Ann. Phys. (Amsterdam) **325**, 2486 (2010); D. D. Ferrante, G. S. Guralnik, Z. Guralnik, and C. Pehlevan, arXiv:1301.4233.
[27] C. M. Bender and S. P. Klevansky, Phys. Rev. Lett. **105**, 031601 (2010). In this reference, it is shown that a $\boldsymbol{\phi}^6$ theory has two different spectra, one for the conventional theory and another for the $\mathcal{PT}$-symmetric theory. A $\boldsymbol{\phi}^{10}$ theory has three spectra, a $\boldsymbol{\phi}^{14}$ has four, and so on.
[28] The spectrum of $H = p^2 - ix$ is null. See I. Herbst, Commun. Math. Phys. **64**, 279 (1979).
[29] These crossing points are exactly analogous to the nonlinear eigenvalues discussed by C. M. Bender, A. Fring, and J. Komijani, J. Phys. A **47**, 235204 (2014).
[30] Square-well m^2 growth of eigenvalues was also found in the large-ϵ behavior of the $x^2(ix)^\epsilon$ $\mathcal{PT}$-symmetric potential. See C. M. Bender, S. Boettcher, H. F. Jones, and V. M. Savage, J. Phys. A **32**, 6771 (1999). In this work, the quantization paths enclosed the negative-imaginary axis as in Fig. 2.